Validation of a novel mechanical model for geometrically and passively confined concrete

Clemens Proksch-Weilguni, Marion Decker, Johann Kollegger

Institute of Structural Engineering, TU Wien, Vienna, Austria

Contact: clemens.proksch-weilguni@tuwien.ac.at

Abstract

Investigating the load-bearing characteristics of the joint region of precast concrete elements under compression is crucial for practical applications, such as in tunnel linings. The study introduces a novel mechanical model to predict the load-bearing capacity of load transfer zones with both geometric confinement caused by load distribution and passive confinement caused by transverse reinforcement. Two design approaches according to the current draft of the Eurocode 2 (EC2) and the novel mechanical model are used for a comparative validation based on experimental tests done at TU Wien and data from literature. The test data relies on centrically loaded test specimens with a simple geometry to exclude side effects which could influence the results regarding geometric and passive confinement. The comparative validation shows the good performance of the novel mechanical model and its advantages in comparison to the models according to the EC2-draft. Due to the mechanical basis, the novel mechanical model can be adapted for more complex geometries and reinforcement layouts for the design of tunnel segments.

Keywords: mechanical model, reinforced concrete, geometric confinement, passive confinement, load-bearing capacity, experimental investigations

1 Introduction

For designing the load transfer zone between two tunnel segments the state of the art according to the current European Standard [1] and the German and Austrian tunneling guidelines [2, 3] is still an approach developed by Spieth in 1959 [4]. This empirical approach, which is presented in Section 2.1, is based on five experimental tests of unreinforced concrete cylinders. The approach has its limitations when it comes to predicting the load-bearing capacity of highly reinforced concrete elements, because it only requires a minimum of transverse reinforcement to cover the tensile splitting forces, which is not directly considered for the prediction. Therefore, the Institute of Structural Engineering developed the **G**eometric and **P**assive **C**onfinement-model (GPC-model [5]) to predict the capacity for load transfer zones, where geometric and passive confinement can be activated. The GPC-model was developed based on mechanical considerations and verified with an experimental campaign of centrically loaded experiments with variable geometric and passive confinement ratios. The test setup to investigate the mechanical effects acting in a load transfer zone is shown in Figure 1. In this article the GPC-model and the two mechanical models according to the new EC2-draft [6] are compared based on experimental data from literature.

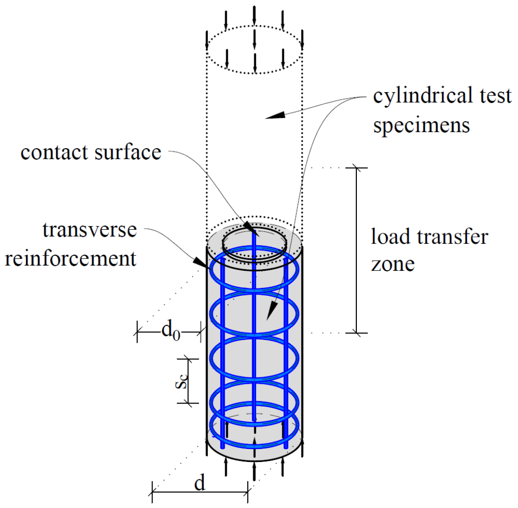

Figure 1. Centrically loaded test specimens, which were used in [5] to verify the GPC-model.

2 Mechanical models

This section presents three models that are used to predict the load-bearing capacity of reinforced concrete elements with a concentrated load introduction. The first two models, which represent the state of the art for the next generation of the European design code, were taken from the EC2-draft [6]. The third one, is the GPC-model which was developed by the research team of the Institute of Structural Engineering at TU Wien. Since the experimental data was chosen based on criteria which insure a failure in the contact surface, this paper focuses on the load-bearing capacity of the contact surface (section 0-0 according to Figure 2). The design procedure for covering the tensile splitting forces in a certain distance of the contact surface (represented by section 1-1 in Figure 2), is discussed in detail in Proksch-Weilguni et al. [5].

2.1 EC2 – Section 8.6 (EC2 approach)

The square root equation in Eqn. (1) (EC2 approach) [6] relies on the ratio of the contact surface area A_{c0} to the area of concrete available for the load distribution A_{c1}. This ratio is used to increase the load-bearing capacity of the uniaxial compressive strength of the contact surface. The load-bearing capacity is verified according to Eqn. (1), which was developed based on experimental tests.

$$F_{cal.EC2} = A_{c0} \cdot f_c \cdot \sqrt{\frac{A_{c1}}{A_{c0}}} \leq 3{,}0 \cdot f_c \cdot A_{c0} \qquad (1)$$

with

f_c	Concrete compressive strength
A_{c0}	Area of the contact surface
A_{c1}	Area of the concrete element available for load distribution

Limiting the load distribution to the same distance in both transverse directions is a requirement for applying Eqn. (1), which is accomplished for the experiments discussed in this study. Additionally, a minimum of transverse splitting reinforcement has to be applied to avoid a failure caused by tensile splitting forces.

2.2 EC2 – Section 8.1.4 (EC2$_{conf}$ approach)

The EC2$_{conf}$-model was originally developed for passively confined concrete structures without a load concentration like regular columns. The new EC2-draft allows to apply the EC2$_{conf}$-model [6], which is presented in the first line of Eqn. (2), for load transfer zones with concentrated load applications. The minimum of the confined concrete area A_{cc} and the contact surface A_{c0} (defined in Figure 2) is decisive for predicting the load-bearing capacity of the contact surface A_{c0}. To consider this aspect when applying EC2$_{conf}$ to load transfer zones, a min-function is applied according to the second line of Eqn. (2). The term to increase the compressive strength caused by passive confinement $\Delta f_{s.cc}$ is applied to the confined concrete area $A_{cc.e}$. To cover the case where the effectively confined concrete area $A_{cc.e}$ is exceeding the dimension of A_{c0}, the second min-function in Eqn. (2) is applied.

$$\begin{aligned} F_{cal.EC2.conf} &= A_{cc} \cdot f_c \cdot + A_{cc.e} \cdot \Delta f_{s.cc} = \\ &= min(A_{cc}; A_{c0}) \cdot f_c \cdot + min(A_{cc.e}; A_{c0}) \cdot \Delta f_{s.cc} \end{aligned} \qquad (2)$$

For circular cross sections the confined concrete area A_{cc} and the effectively confined concrete area $A_{cc.e}$ can be determined according to Eqn. (3) and Eqn. (4).

$$A_{cc} = \frac{\pi}{4} \cdot {d_c}^2 \tag{3}$$

$$A_{cc.e} = \frac{\pi}{4} \cdot \left(d_c - \frac{s_c}{2}\right)^2 \tag{4}$$

The term $\Delta f_{s.cc}$ considers the compressive strength increase due to steel confined concrete and should be calculated according to Eqn. (5).

$$\Delta f_{s.cc} = \begin{cases} 4 \cdot \sigma_{cc} & \text{for} \quad \sigma_{cc} \leq 0{,}6 f_c \\ 3{,}5 \cdot {\sigma_{cc}}^{3/4} \cdot {f_c}^{1/4} & \text{for} \quad \sigma_{cc} > 0{,}6 f_c \end{cases} \tag{5}$$

Eqn. (6) has to be used to compute the transverse compressive stress σ_{cc} resulting from the transverse reinforcement. The cross-sectional area of a transverse reinforcing layer is called A_s therein.

$$\sigma_{cc} = \frac{A_s \cdot f_y}{s_c \cdot d_c} \tag{6}$$

with

A_s Cross-sectional area of a transverse reinforcement layer

f_y Yield strength of reinforcement

s_c Spacing between the transverse reinforcement bars in the discontinuity region

2.3 Geometric and passive confinement - model (GPC - model)

The GPC-model was developed for load transfer zones in reinforced concrete structures including a load distribution and a transverse reinforcement. In Proksch-Weilguni et al. [5] the development of the GPC-model is presented including the possibility to check the load bearing-capacity in two sections of the load transfer zone. This paper focuses on the load-bearing capacity of the contact surface (section 0-0).

Eqn. (7) divides the load-bearing capacity of a geometrically and passively confined contact surface into three parts. The first term F_{cm} relates to the uniaxial concrete compressive strength f_{cm}. The second term ΔF_c takes the geometric confinement effect into account. The third term $\Delta F_{s.cc}$ takes into account the increase in strength caused by the transverse reinforcement (passive confinement).

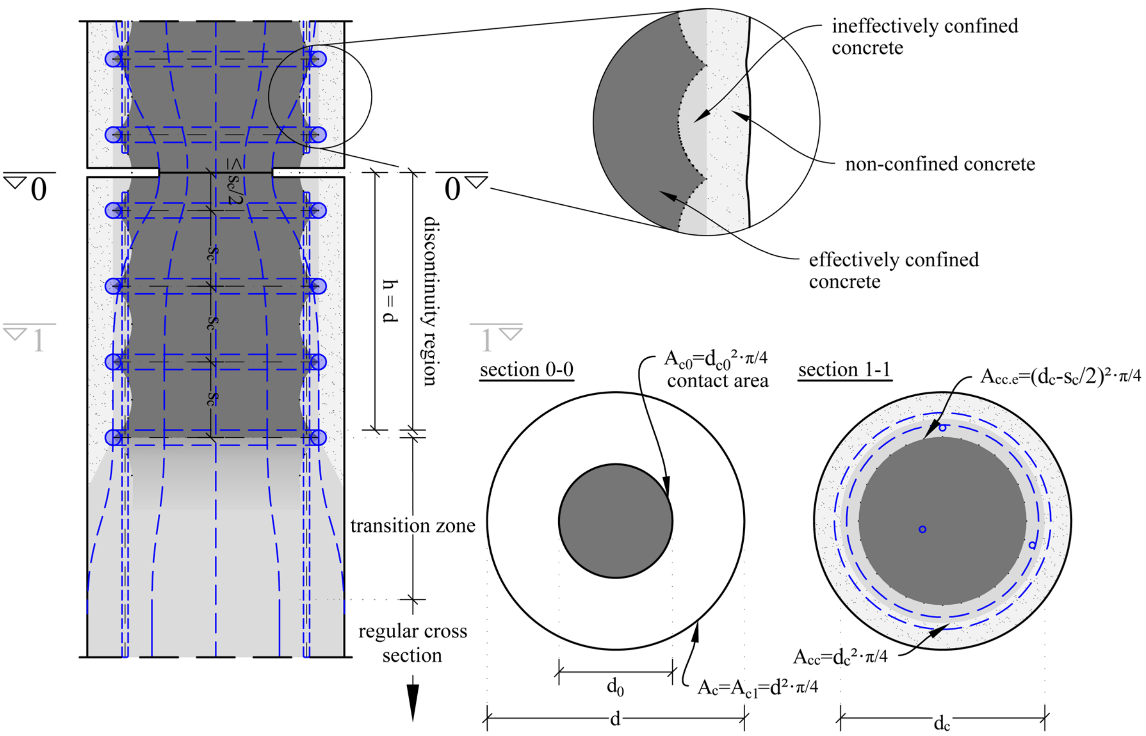

Figure 2. Mechanical effects and their simplifications acting in a load transfer zone (taken and adopted from [5])

$$F_{cal.GPC0} = F_{cm} + \Delta F_c + \Delta F_{s.cc} = \\ = f_{cm} \cdot A_{c0} + \Delta f_c \cdot A_{c0} \\ + \Delta f_{s.cc} \cdot min(A_{c0}; A_{cc.e}) \quad (7)$$

Regarding the effect of the load distribution Eqn. (8) proposes an empirical function to capture the increase in concrete strength, which is based on Spieth's fundamental experiments [4, 7]. The innovation in Eqn. (8) is the use of A_{cc} instead of A_c based on the consideration that the load distribution only occurs in the confined concrete (effectively confined + ineffectively confined concrete according to Figure 2) when reaching the peak load.

$$\Delta f_c = f_{cm} \cdot \left(\left(\frac{A_{cc}}{A_{c0}} \right)^{1/2} - 1 \right) \quad (8)$$

The term to increase the compressive strength due to passive confinement is calculated according to Eqn. (5) and Eqn. (6).

3 Comprehensive validation

In this section data from literature, including 24 experiments carried out at TU Wien [5] and 40 external experiments [8], is used for a comprehensive validation of the bearing capacity predictions of the EC2-model, the $EC2_{conf}$-model and the GPC-model. The range of the investigated parameters covers a mechanical reinforcement ratio of ω = 0.07 to 0.470 and a load concentration ratio of A_{cc}/A_{c0} = 1.18 to 9.0. The experimental data and the load-bearing capacity predictions are enclosed in Table 1 of the Appendix.

The two parameters, which this study focuses on, are the load distribution and the impediment of lateral expansion by reinforcement. Furthermore the load-bearing capacity of concrete elements can be affected by a number of factors, including the load introduction system, the slenderness of the specimens and inadequate splitting reinforcement. The test specimen design must satisfy the following requirements in order to be chosen for the validation:

- Centric loading of the specimens is required.
- Section 0–0, as shown in Figure 2, should be decisive for failure as geometric and passive confinement effects have to be activated when reaching the failure load.
- Detailed information of the geometric and mechanical characteristics must be accessible in order to exclude the possibility that splitting forces will cause an early failure.
- A minimum ratio of H/d is required for excluding side effects in the discontinuity area adjacent to the contact surface.
- The reinforcement geometry has to be circular shaped.

Experimental data, that satisfy all of these requirements are rare in literature. Therefore, also experiments which were performed with steel plates for load introduction were considered for the validation. The comparative validation is shown in Figure 3, where the experimental data is compared with the predicted load-bearing capacities according to the mechanical models mentioned in Section 2. The horizontal red line indicates the ideal prediction.

The EC2-model, which only considers the geometric confinement effect, is not able to cover situations with an increasing reinforcement ratio (shown in Figure 3a). This leads to empirically determined capacities that are up to 2.1 times higher than the predicted ones, which can be seen in Figure 3a and 3b. The mean value of the ratio between $F_{exp}/F_{cal.EC2}$ is 1.48 and the variation coefficient 16%.

The $EC2_{conf}$ approach covers various situations of passive confinement but does not make accurate predictions when the ratio A_{cc}/A_{c0} is increased. This trend can be seen by comparing the inclination of the 1st order polynomial fit in Figure 3c and 3d. The mean value of the ratio between $F_{exp}/F_{cal.EC2conf}$ is 1.64 and the variation coefficient is 29%. The deficits of both EC2-models can be compensated with the GPC-model, which can be seen in Figure 3e and 3f, where the model yields accurate results along the whole spectrum of practically relevant reinforcement ratios and load concentration ratios. The mean ratio between $F_{exp}/F_{cal.GPC}$ of 1.18 and a variation coefficient of 13% confirm the good performance of the GPC-model.

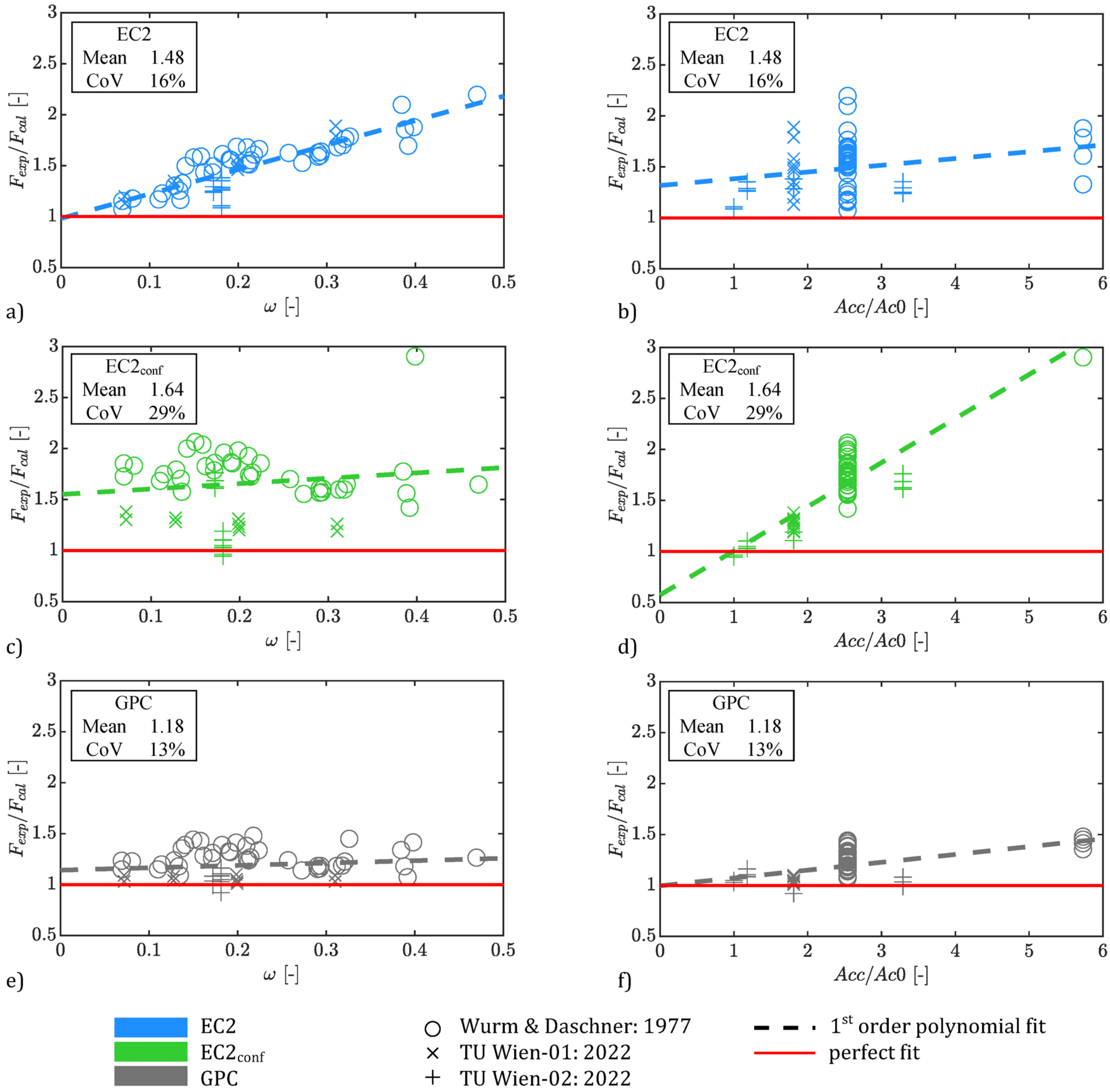

Figure 3. Ratio of experimental and predicted load-bearing capacities as a function of the transverse mechanical reinforcement ratio ω [-] and the load concentration ratio A_{cc}/A_{c0}

4 Conclusion

The goal of this research was to compare three mechanical models which can be used for the prediction of the capacity of load transfer zones with practical boundary conditions regarding the transverse reinforcement ratio and the load concentration ratio. The literature validation of the geometric and passive confinement-model (GPC-model) results in a mean ratio between F_{exp} and $F_{cal.GPC}$ of 1.18 and a variation coefficient of 13%, which is more accurate than the validation of the EC2-model and the EC2$_{conf}$-model.

The possibility of a precise prediction using the GPC-model results into a safe design and enables resource-efficient reinforcement layouts for load transfer zones. The mechanical foundation of the GPC-model allows it to be modified for more complex reinforcement layouts and geometries. The simple analysis procedure of the model has the potential to be widely applied by practitioners in the future.

Authorship contribution

Clemens Proksch-Weilguni: Formal analysis, Methodology, writing – conceptualization, preparation of the original draft. **Marion Decker:** Methodology, review & editing. **Johann Kollegger:** Review & editing, supervision, funding acquisition.

References

[1.] ÖNORM EN 1992-1-1 Design of concrete structures: Part 1-1: General rules and rules for buildings. Vienna: Austrian Standards Institute, 2015.

[2.] ÖVBB Tübbingsysteme aus Beton Wien: Österreichische Vereinigung für Beton- und Bautechnik, 2009.

[3.] DAUB Empfehlungen für den Entwurf, die Herstellung und den Einbau von Tübbingringen Köln: Deutscher Ausschuss für unterirdisches Bauen, 2013.

[4.] Spieth H.-P., *Das Verhalten von Beton unter hoher örtlicher Pressung und Teilbelastung unter besonderer Berücksichtigung von Spannbetonverankerungen*. Technische Hochschule Stuttgart: Stuttgart, 1959.

[5.] Proksch-Weilguni C., Decker M., and Kollegger J. Load distribution and passive confinement in reinforced conrete: Development of a mechanical model. Engineering Structures. 2024;304(117562).

[6.] ÖNORM FprEN 1992-1-1 Design of concrete structures - Part 1-1: General rules - Rules for buildings, bridges and civil engineering structures; FprEN 1992-1-1:2023. Brussels: European Commitee for Standardization, 2023.

[7.] Spieth H.-P. Das Verhalten von Beton unter hoher örtlicher Pressung. Beton- und Stahlbetonbau. 1961;56(Heft 11):257-262.

[8.] Wurm P. and Daschner F. Versuche über Teilflächenbelastung von Normalbeton (DAfStb Heft 286). Technische Univeristät München: Verlag von Wilhelm Ernst & Sohn; 1977.

Appendix

Table 1. Experiments used for the comprehensive validation

General information		Specimen properties				Results			
Source	Name	ω_{regel}	A_{cc} / A_{c0}	f_{cm}	f_{ym}	F_{exp}	F_{exp}/ $F_{cal.EC2}$	F_{exp}/ $F_{cal.EC2conf}$	F_{exp}/ $F_{cal.GPC}$
		[-]	[-]	[N/mm²]	[N/mm²]	[kN]	[-]	[-]	[-]
Wurm:1977	16 (III D)	0.1983	2.54	26.1	374	1980.0	1.69	1.98	1.41
	22 (III D)	0.1903	2.54	27.2	374	1912.0	1.56	1.87	1.33
	28 (III D)	0.1917	2.54	27.0	374	1892.0	1.56	1.85	1.32
	15 (III C)	0.1710	2.54	27.5	286	1775.0	1.43	1.79	1.26
	21 (III C)	0.1717	2.54	27.4	286	1843.0	1.49	1.86	1.31
	27 (IIIC)	0.1823	2.54	25.8	286	1873.0	1.61	1.96	1.39
	13 (III A)	0.2099	2.54	27.5	282	2079.0	1.68	1.93	1.38
	19 (III A)	0.2106	2.54	27.4	282	1873.0	1.52	1.74	1.25
	25 (III A)	0.2237	2.54	25.8	282	1931.0	1.66	1.86	1.34
	14 (III B)	0.2926	2.54	27.5	325	1981.0	1.60	1.57	1.16
	20 (III B)	0.2937	2.54	27.4	325	2020.0	1.64	1.61	1.18
	26 (III B)	0.3119	2.54	25.8	325	1952.0	1.68	1.60	1.18
	36 (IV B)	0.0806	2.54	25.9	280	1373.0	1.18	1.83	1.23
	37 (IV B)	0.0692	2.54	30.2	280	1461.0	1.08	1.73	1.15
	38 (IV B)	0.0692	2.54	30.2	280	1569.0	1.15	1.85	1.23
	35 (IV B)	0.1283	2.54	25.9	291	1520.0	1.30	1.79	1.24

	39 (IV B)	0.1100	2.54	30.2	291	1589.0	1.17	1.68	1.15
	40 (IV B)	0.1142	2.54	29.1	291	1608.0	1.23	1.75	1.20
	33 (IV B)	0.1499	2.54	27.3	239	1942.0	1.58	2.06	1.44
	34 (IV B)	0.1580	2.54	25.9	239	1853.0	1.59	2.04	1.43
	41 (IV B)	0.1406	2.54	29.1	239	1961.0	1.50	2.00	1.39
	31 (IV B)	0.2903	2.54	27.3	250	2001.0	1.63	1.61	1.18
	32 (IV B)	0.2903	2.54	27.3	250	1952.0	1.59	1.57	1.15
	42 (IV B)	0.2723	2.54	29.1	250	2001.0	1.53	1.55	1.14
	115 (XIII)	0.1615	2.54	26.7	486	1726.0	1.44	1.83	1.28
	116 (XIII)	0.1348	2.54	32.0	486	1677.0	1.16	1.58	1.09
	117 (XIII)	0.1335	2.54	32.3	486	1824.0	1.25	1.70	1.18
	119 (XIII)	0.2569	2.54	26.7	495	1952.0	1.62	1.70	1.24
	120 (XIII)	0.2144	2.54	32.0	495	2236.0	1.55	1.76	1.27
	121 (XIII)	0.2124	2.54	32.3	495	2197.0	1.51	1.72	1.24
	123 (XIII)	0.3846	2.54	26.7	515	2520.0	2.10	1.77	1.34
	124 (XIII)	0.3209	2.54	32.0	515	2540.0	1.76	1.65	1.23
	125 (XIII)	0.3179	2.54	32.3	515	2471.0	1.70	1.60	1.19
	127 (XIII)	0.4697	2.54	26.7	462	2638.0	2.20	1.65	1.26
	128 (XIII)	0.3919	2.54	32.0	462	2442.0	1.70	1.42	1.07
	129 (XIII)	0.3882	2.54	32.3	462	2697.0	1.86	1.56	1.18
	118 (XIV)	0.1369	5.73	31.5	486	1255.0	1.33	3.01	1.35
	122 (XIV)	0.2178	5.73	31.5	495	1520.0	1.61	3.19	1.48
	126 (XIV)	0.3260	5.73	31.5	515	1687.0	1.79	3.02	1.45
	130 (XIV)	0.3981	5.73	31.5	462	1775.0	1.88	2.90	1.41
Proksch 2022 (TU Wien 01)	A1-V1	0.1985	0.82	48.0	580	1154.0	1.36	1.07	1.07
	A1-V2	0.1985	0.82	48.0	580	1151.0	1.36	1.06	1.06
	C1-V1	0.0718	1.81	48.0	580	645.8	1.13	1.30	1.03
	C1-V2	0.0718	1.81	48.0	580	684.3	1.20	1.38	1.09
	D1-V1	0.1276	1.81	48.0	580	769.4	1.35	1.32	1.08
	D1-V2	0.1276	1.81	48.0	580	744.5	1.30	1.28	1.04
	E1-V1	0.1994	1.81	48.0	580	832.3	1.46	1.20	1.01
	E1-V2	0.1994	1.81	48.0	580	851.0	1.49	1.23	1.03
	F1-V1	0.1985	1.81	48.0	580	867.0	1.52	1.26	1.05
	F1-V2	0.1985	1.81	48.0	580	902.0	1.58	1.31	1.10
	G1-V1	0.3101	1.81	48.0	580	1021.6	1.79	1.19	1.03
	G1-V2	0.3101	1.81	48.0	580	1082.1	1.89	1.26	1.09
Proksch 2022 (TU Wien 02)	H2-V1	0.1812	0.82	52.8	580	1033.0	1.11	0.96	0.96
	H2-V2	0.1812	0.82	52.8	580	1014.0	1.09	0.94	0.94
	I2-V1	0.1812	1.18	52.8	580	980.0	1.26	1.03	0.97
	I2-V2	0.1812	1.18	52.8	580	985.0	1.27	1.03	0.97
	J2-V1	0.1812	1.81	52.8	580	868.0	1.38	1.19	0.99
	J2-V2	0.1812	1.81	52.8	580	807.0	1.28	1.11	0.92
	K2-V1	0.1721	3.29	55.6	580	614.0	1.25	1.63	1.00
	K2-V2	0.1721	3.29	55.6	580	608.0	1.24	1.61	0.99
	I2a-V1	0.1812	1.18	52.8	580	1052.0	1.35	1.10	1.04
	I2a-V2	0.1812	1.18	52.8	580	1001.0	1.29	1.05	0.99
	K2a-V1	0.1721	3.29	55.6	580	665.0	1.35	1.76	1.08
	K2a-V2	0.1721	3.29	55.6	580	636.0	1.29	1.68	1.03